

**NANOCOMPOSITES:
A REVOLUTIONARY NEW FLAME RETARDANT APPROACH**

Jeffrey W. Gilman*, Takashi Kashiwagi
National Institute of Standards and Technology
Gaithersburg, MD

Joseph D. Lichtenhan
Phillips Laboratory
Edwards Air Force Base, CA

ABSTRACT

To evaluate the feasibility of controlling polymer flammability via a nanocomposite approach, we have examined the flammability properties of nylon-6 clay nanocomposites. The fire retardant (FR) properties of this new class of materials, organic - inorganic nanocomposites, are reported. The Cone calorimeter data show that the peak heat release rate (HRR), the most important parameter for predicting fire hazard, is reduced by 63 % in a nylon-6 clay-nanocomposite containing a clay mass fraction of only 5 %. Not only is this a very efficient FR system but it does not have the usual drawbacks associated with other FR additives. That is, the physical properties are not degraded by the additive (clay), instead they are greatly improved. Furthermore, this system does not increase the carbon monoxide or soot produced during the combustion, as many commercial fire retardants do. The nanocomposite structure appears to enhance the performance of the char through reinforcement of the char layer. Indeed, transmission electron microscopy (TEM) of a section of the combustion char from the nylon-6 clay-nanocomposite (5 %) shows a multilayered silicate structure. This layer may act as an insulator and a mass transport barrier slowing the escape of the volatile products generated as the nylon-6 decomposes.

KEY WORDS: Nanocomposite, Flammability, Clay.

1. INTRODUCTION

In the pursuit of improved approaches to fire retarding polymers a wide variety of concerns must be addressed, in addition to the flammability issues. For commodity polymers the low cost of these materials requires that the fire retardant (FR) approach also be of low cost. This limits the solutions to the problem primarily to additive type approaches. These additives

must be low cost and easily processed with the polymer. In addition, any additive must not excessively degrade the other performance properties, and it must not create environmental problems in terms of recycling or disposal of the final product. However, currently available flame retardant approaches for nylon tend to reduce the thermal and mechanical properties of the nylon (1,2).

Nylon-6 clay nanocomposites, first developed by researchers at Toyota Central Research and Development Laboratories, are hybrid organic polymer - inorganic materials with unique properties when compared to conventional filled polymers. The nylon-6 clay nanocomposites (clay mass fractions from 2 % to 70 %) are synthesized by ring-opening polymerization of ϵ -caprolactam in the presence of cation exchanged montmorillonite clay (3). The layered silicate structure of the montmorillonite clay is represented in Figure 1. This process creates a polymer layered silicate nanocomposite with either a delaminated hybrid structure or an intercalated hybrid structure (see Figure 2). The intercalated structure, which forms when the mass fraction of clay is greater than 20 %, is characterized by a well ordered multilayer with spacing between the silicate layers of only a few nanometers. The delaminated hybrid structure, which forms when the mass fraction of clay is less than 20 %, contains the silicate layers individually dispersed in the polymer matrix (4). The mechanical properties for the nylon-6 clay nanocomposite with 5 % clay mass fraction show excellent improvement over pure nylon-6. The nanocomposite exhibits a 40 % higher tensile strength, 68 % greater tensile modulus, 60 % higher flexural strength, 126 % increased flexural modulus, and comparable Izod and Charpy impact strengths. The heat distortion temperature (HDT) is increased from 65° C (nylon-6) to 152° C (nylon-6 clay nanocomposites with clay mass fractions \geq 5 %) (5). To evaluate the feasibility of controlling polymer flammability via a nanocomposite approach, we have examined the flammability properties of nylon-6 clay nanocomposites with clay mass fractions of 2 % and 5 %, and compared them to those for pure nylon-6, and other flame retarded nylons.

2. EXPERIMENTAL

All nylon-6 clay nanocomposites (clay mass fraction of 2 % and 5 %) and nylon-6 were obtained from UBE industries and used as received (6). The above nanocomposites will be referred to as; nylon-6 clay nanocomposite (2%) and nylon-6 clay nanocomposite (5%), respectively. Evaluations of flammability were done using the Cone Calorimeter (7). The tests were done at an incident heat flux of 35 kW/m² using the cone heater. A heat flux of 35 kW/m² represents a typical small-fire scenario (8). Peak heat release rate, mass loss rate and specific extinction area (SEA) data, measured at 35 kW/m², are reproducible to within \pm 15 %. The carbon monoxide and heat of combustion data are reproducible to within \pm 10 %. The uncertainties for the Cone calorimeter are based on the uncertainties observed while evaluating the thousands of samples combusted to date. Cone samples were prepared by compression molding the samples (~55 g) into 75 mm x 50 mm rectangular plaques, 15 mm thick, using a press with a heated mold. The thermogravimetric analysis was done on a Perkin-Elmer 7 Series TGA. Four runs of each sample type were typically run, the results averaged and the uncertainties calculated using standard methods. For the differential TGA plots (Figure 5) the uncertainty in $d(m/m_0)/dT$ ($^{\circ}C^{-1}$), of the $d(m/m_0)/dT$ versus temperature plot, was found to be \pm 20 % (\pm 1 standard deviation) and the uncertainty in the temperature at the maximum, in the $d(m/m_0)/dT$ versus temperature plot, was found to be \pm 2 % (\pm 1 standard deviation). These uncertainties are shown as "error bars" on data points at 390° C and 460° C, in Figure 5. For the transmission electron microscopy (TEM), the char was broken into small pieces, embedded in an epoxy resin (Epofix), and cured overnight at room temperature. Ultra-thin sections were prepared with a 45° diamond knife at room temperature using a DuPont-Sorvall 6000 ultramicrotome. Thin sections (nominally 50 nm-70 nm) were floated onto water and mounted on 200-mesh carbon-

coated copper grids. Bright-field TEM images were obtained with a Philips 400T microscope operating at 120 kV, utilizing low-dose techniques. Microscale Combustion data were obtained using a custom built system developed by Lyon and Walters, details of which are reported elsewhere in these proceedings.

3. RESULTS AND DISCUSSION

3.1. CONE CALORIMETER

3.1.1 Heat Release Rate. The heat release rate (HRR) data from the Cone Calorimeter for nylon-6, nylon-6 clay-nanocomposite (2 %), and nylon-6 clay-nanocomposite (5 %) when exposed to a 35 kW/m² heat flux, are shown in Figure 3. The clay-nanocomposites reduce the peak HRR of nylon-6 by 32 % and 63 %, respectively. The fraction of clay present in the nanocomposite, at these levels, is directly proportional to the reduction in HRR. The peak heat release rate has been shown to be the most important parameter for predicting fire hazard.

3.1.2 Char Formation and Characterization. Visual observations of the combustion experiments, in the Cone calorimeter, reveals different behavior for the nylon-6 clay-nanocomposites, compared to the pure nylon-6, from the very beginning of the thermal exposure. A thin char layer forms, on the top of all the samples, in the first several minutes of exposure, prior to ignition. In the case of pure nylon-6, this char layer fractures into small pieces early in the combustion. The char does not fracture with the nylon-6 clay-nanocomposites. This tougher char layer survives and grows throughout the combustion, yielding a rigid multicellular char-brick with the same dimensions as the original sample. The HRR curves for the nylon-6 clay-nanocomposites show the double maxima characteristic of material that forms a char layer during combustion (9). The nanocomposite structure appears to enhance the performance of the char through reinforcement of the char layer. Preliminary, TEM of a section of the combustion char from the nylon-6 clay-nanocomposite (5 %) is shown in Figure 4. A multilayered silicate structure is seen after combustion, with the darker, 1 nm thick, silicate sheets forming a large array of fairly even layers. This was the primary morphology seen in the TEM of the char, however, some voids were also present. At this clay content (5 %), the original nanocomposite contains mostly the delaminated structure (3, 5), this implies that the layered structure seen in the TEM formed during combustion. The delaminated hybrid structure, which subsequently collapses during combustion, may act as an insulator and a mass transport barrier, slowing the escape of the volatile products generated as the nylon-6 decomposes. An additional explanation, proposed by Giannelis et. al., after they observed self-extinguishing behavior of a polycaprolactone nanocomposite, attributes the low flammability to the excellent barrier properties of the nanocomposite. The nanocomposites low permeability for liquids and gases may slow the transport of volatile fuel through the nanocomposite and into the gas phase (10). Further X-ray and TEM analysis of the char and the original nylon-6 nanocomposite structure are underway to better understand the flammability behavior.

3.1.3 Thermal Stability. The differential thermogravimetric analysis (DTGA) data, comparing the nylon-6 thermal stability to that for the nylon-6 clay-nanocomposite (5 %), are shown in Figure 5. Surprisingly, within the uncertainty of the data, there is little apparent difference in thermal stability. Therefore, it is not likely that the reduced flammability is due to a higher thermal stability of the nanocomposites compared to the pure nylon-6. Moreover, analysis of the samples using the Microscale Combustion Calorimeter, developed by Lyon and Walters (11), yielded a similar result. This calorimeter couples a thermogravimetric analysis instrument with a gas-phase flow combustion system. The microscale calorimeter rapidly (>200 K/min) heats a milligram size sample to a constant, calibrated heat flux, in the TGA under an inert atmosphere, and then burns the pyrolysis gases in excess oxygen at high temperature. As Figure 6 shows, there is no apparent difference in the "micro-heat release rate" (μ HRR) data for these materials. This is probably due to the fact that this system measures the intrinsic thermal stability of a material and is insensitive to effects which only occur at larger scale.

3.1.4 Heat of Combustion, Carbon Monoxide and Smoke. Most fire retardants function by one of the following mechanisms; 1) by changing the condensed phase

chemistry, which usually results in the formation of a char, 2) by altering the gas phase chemistry, 3) by endothermically cooling the material, or 4) through some combination of these. Some of the more effective fire retardants (by mass fraction), such as halogen and some phosphorus based systems, reduce polymer flammability by their ability to form gaseous intermediates which scavenge flame propagating free radicals (e.g., OH and H) thereby inhibiting complete combustion to CO₂. The result is to lower the heat of combustion of the polymer/fire retardant formulation and lower the HRR. An inherent drawback to the gas phase flame retardant approach, is that an increase in the yields of carbon monoxide (CO) and soot are usually observed. In some cases, depending on how effective the system is at reducing the HRR, this can also increase the rate of CO and smoke generation (12). This is undesirable since CO and smoke (the combination of soot and combustion gases) are the primary cause of death in most fires (13).

A comparison of the heats of combustion for nylon-6, nylon-6 clay-nanocomposite (2 %), and nylon-6 clay-nanocomposites (5 %), is shown in Figure 7. These data show that the nylon-6 clay-nanocomposites (2%) and (5%) have the same heats of combustion as nylon-6. The specific extinction area (SEA) data (a measure of soot) for nylon-6 and nylon-6 clay-nanocomposite (5 %) are shown in Figure 8 and Table 1. The nanocomposite has about a 50 % greater mean SEA than pure nylon-6. Figure 9 and Table 1 show the CO yield data for nylon-6 and nylon-6 clay-nanocomposite (5 %). Here we observe a factor of two increase in the CO yield for the nanocomposite. This type of behavior may be due to a small increase in the concentration of olefinic or aromatic compounds present in the gas phase. Typically, the SEA yield is much more sensitive to the level of olefinic or aromatic compounds than the heat of combustion is. Hamins et. al. found an increase in soot levels in methane flames when only 1 mole % of toluene was added to the fuel (14). Possibly, the silicate is catalyzing the formation of olefinic or aromatic compounds, i.e., through dehydrogenation reactions, during the decomposition in the condensed phase. Furthermore, recent thermal decomposition studies have shown that nylon-6 produces CO during pyrolysis in inert atmospheres (15). The silicate may also be catalyzing this process. Since, there is no change in the heat of combustion and only relatively small changes in the SEA and CO yields, it is reasonable to conclude that the nanocomposites' lower HRR are from changes in the condensed phase decomposition processes and not from a gas phase effect.

Figure 10 shows the mass loss rate data for nylon-6, nylon-6 clay-nanocomposite (2 %), and nylon-6 clay-nanocomposites (5 %). The three curves closely resemble the HRR curves (Figure 3), indicating that the reduction in HRR for the nanocomposites is primarily due to the reduced mass loss rate and the resulting lower fuel feed rate to the gas phase. To evaluate the fire safety of a flame retarded material it is useful to examine the rate of soot and CO generation instead of just the soot and CO yield. The extinction rate (m²/s) (Figure 11) is obtained from the product of the SEA (m²/kg) and the mass loss rate (kg/s). The CO production rate (kg/s) (Figure 12) is obtained from the product of the CO yield (kg/kg) and the mass loss rate (kg/s). The lower mass loss rates give lower rates of soot generation, and similar CO production rates, during the combustion of the nanocomposites, as compared to the pure nylon-6. The nanocomposites are therefore, fire safe materials in terms of HRR, soot and CO production.

4. OTHER FLAME RETARDANT APPROACHES

Comparison of the nylon-6 clay-nanocomposites to other flame retarded nylon systems, such as a nylon-6,6 triphenylphosphine oxide copolymer (nylon-6,6-PO), where the flame retardant is also combined with the nylon at the molecular level, further illustrates the unique benefits the nanocomposite approach offers. Table 1 shows that the nylon-6,6-PO copolymer gives a similar reduction in HRR (58 %) to that for the nanocomposite (63 %) at a comparable level of incorporation of "flame retardant" (4 % mass fraction of phosphorus). The phosphine oxide copolymer appears to function by increasing the amount of char formed (8.5 %) and by reducing the heat of combustion (by 40 %). Unfortunately, for the reasons explained above for flame retardants which act on the gas phase combustion processes, the SEA is seven times greater, and the CO yield is increased by 16 fold (16). Even though the mass loss rate for the copolymer is 50 % lower than that for pure nylon-6,6, the extinction rate is still 4 times greater, and the CO rate is still 10 times greater, than that for pure nylon-

6.6. Another additive FR system for nylon, based on ammonium polyphosphate (APP), requires ≥ 35 % mass fraction of additive to significantly effect the flammability (measured by oxygen index) of nylon-6, and, as mentioned in the introduction, this results in as much as a 20 % loss of mechanical properties. Finally, it should be noted that the nano-dispersed clay composite structure has a very different effect on the flammability of nylon than macro- or meso-dispersed clay-polymer mixtures. Bourbigot and Le Bras found, in their extensive study of clays in an intumescent polypropylene system, that montmorillonite clay, similar to the ion exchanged montmorillonite clay used to make the nylon nanocomposite, actually decreased the limiting oxygen index, i.e., increased the flammability of the intumescent polypropylene (17).

5. FUTURE WORK

The ring-opening catalyzed synthesis, by which the nylon-6 clay-nanocomposites are prepared, yields the delaminated structure shown in Figure 2. In this structure the ammonium end group on the nylon-6 interacts ionically with the anionic silicate layer. Characterization of the nylon-6 clay-nanocomposites (2 % and 5 %) by Usuki et al., revealed that 30 % and 50 %, respectively, of the nylon-6 polymer chains were "bound" to the silicate through this interaction. It is possible that it is only this fraction of the nylon that imparts the superior flammability and mechanical properties. Other polymer silicate nanocomposites based on a wide variety of resins, such as polystyrene, epoxy, poly(ethylene oxide), polysiloxane, polyesters, and polyphosphazenes, have recently been prepared via melt intercalation (18). These materials possess varying degrees of interaction between the polymer and the silicate layer and provide the opportunity to study the effect this variable has on flammability and to determine if the clay-nanocomposite approach is useful in reducing the flammability of other polymers. We are continuing to investigate the mechanism of flame retardancy in clay and other nanocomposite materials.

6. CONCLUSIONS

The fire retardant (FR) properties of nylon-6 clay-nanocomposites, are reported. The peak heat release rate (HRR) is reduced by 63 % in a nylon-6 clay-nanocomposite containing a clay mass fraction of only 5 %. Not only is this a very efficient FR system but it does not have the usual drawbacks associated with other FR additives. That is, the physical properties are not degraded by the additive (clay), instead they are greatly improved. Furthermore, this system does not increase the carbon monoxide or soot produced during the combustion, as many commercial fire retardants do. The nanocomposite structure appears to enhance the performance of the char through reinforcement of the char layer. Indeed, transmission electron microscopy (TEM) of a section of the combustion char from the nylon-6 clay-nanocomposite (5 %) shows a multilayered silicate structure. This layer may act as an insulator and a mass transport barrier slowing the escape of the volatile products generated as the nylon-6 decomposes.

7. ACKNOWLEDGMENTS

The authors (J.G. and T. K.) would like to thank the Federal Aviation Administration for partial funding of this work, through Interagency Agreement DTFA0003-92-Z-0018. We would also like to thank Mr. Jack Lee (NIST) for Cone Calorimeter analysis. Dr. Catheryn Jackson (NIST) and Dr. Henri Chanzy (NIST) for TEM analysis of the char samples. Dr. M. Nyden (NIST) and Dr. E. Manias (Cornell University) for the montmorillonite structure, Dr. R. Lyon (FAA) and Mr. R Walters (FAA) for micro calorimeter analysis and Professor E. Giannelis (Cornell University) for helpful discussions.

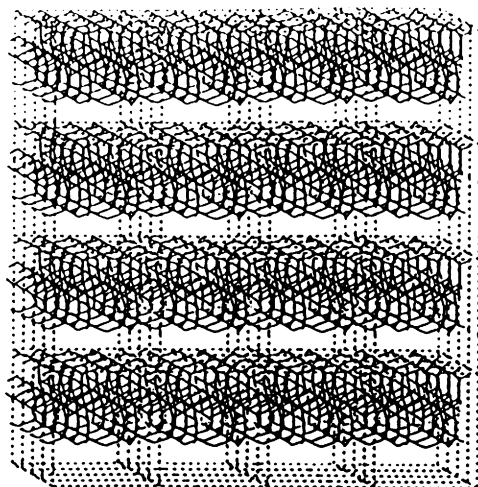


Figure 1. Representation of the montmorillonite clay structure showing the silicate layers and the interlayer gap or gallery.

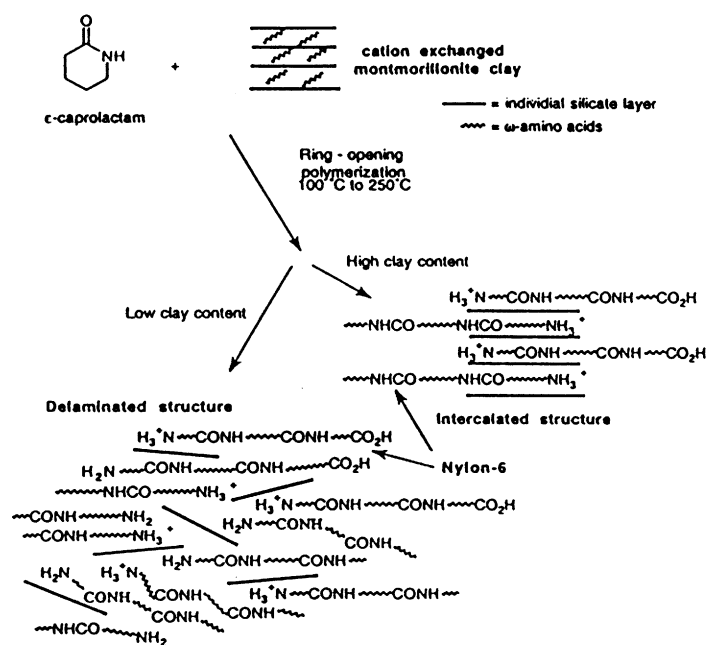


Figure 2. Diagram of the process used to prepare polymer layered silicate nanocomposites with either a delaminated hybrid structure or an intercalated hybrid structure.

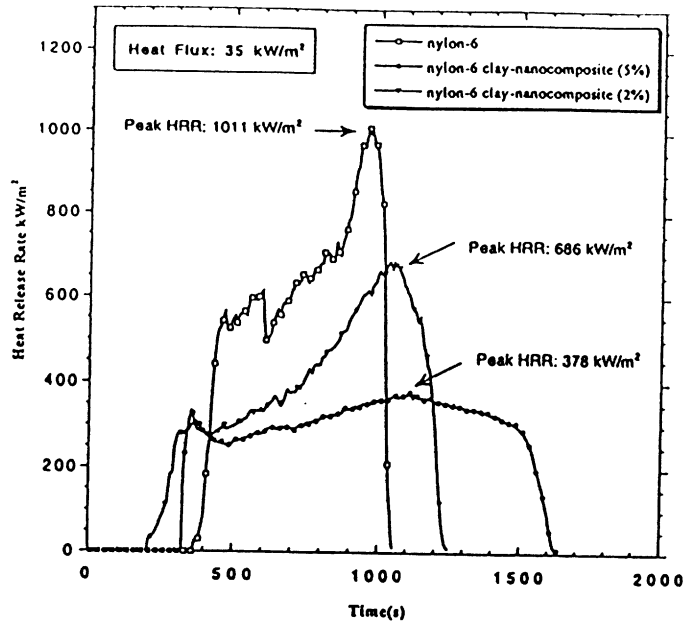


Figure 3. Comparison of the Heat Release Rate (HRR) plot for nylon-6, nylon-6 clay-nanocomposite (mass fraction 2 %) and nylon-6 clay-nanocomposite (mass fraction 5 %) at 35 kW/m² heat flux, showing respectively, the 32 % and 63 % reduction in HRR's for the nanocomposites.

Table 1. Cone Calorimeter Data

Sample	Residue Yield (%) ± 0.3	Peak HRR (kW/m ²) (% decrease) ± 15%	Mean Heat of Combustion (MJ/kg) ± 10%	Total Heat Released (MJ/m ²) ± 10%	Mean Specific Extinction Area (m ² /kg) ± 10%	Mean CO yield (kg/kg) ± 10%
Nylon-6	0.3	1011	27	413	197	0.01
Nylon-6 clay-nano-composite 2%	3.4	686 (32%)	27	406	271	0.01
Nylon-6 clay-nano-composite 5%	5.5	378 (63%)	27	397	296	0.02
Nylon-6,6	0	1190	30	95	200	0.01
Nylon-6,6 -PO 4% Phosphorus	8.5	490 (58%)	18	50	1400	0.16

* TGA char yield in air, 10° C/minute, uncertainty ± 2 %



Figure 4. TEM of a section of the combustion char from the nylon-6 clay-nanocomposite (5 %) showing the silicate (1 nm thick, dark bands) multilayered structure.

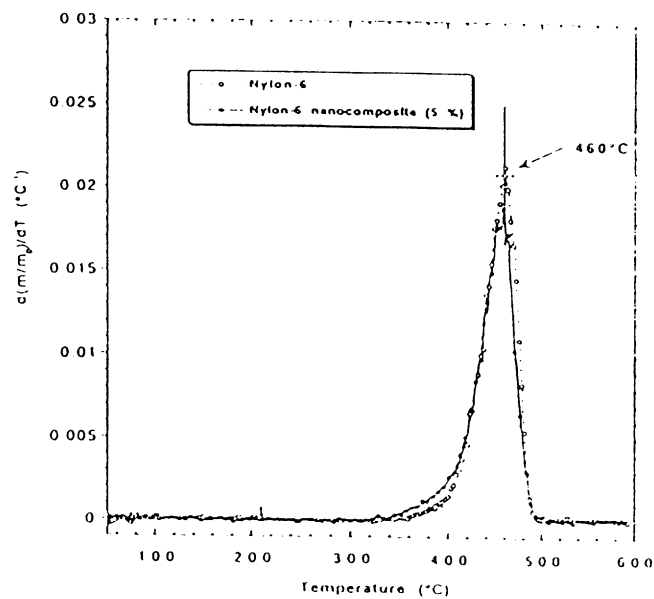


Figure 5. Comparison of the derivative of the TGA curves for nylon-6 and the nylon-6 clay-nanocomposite (5 %).

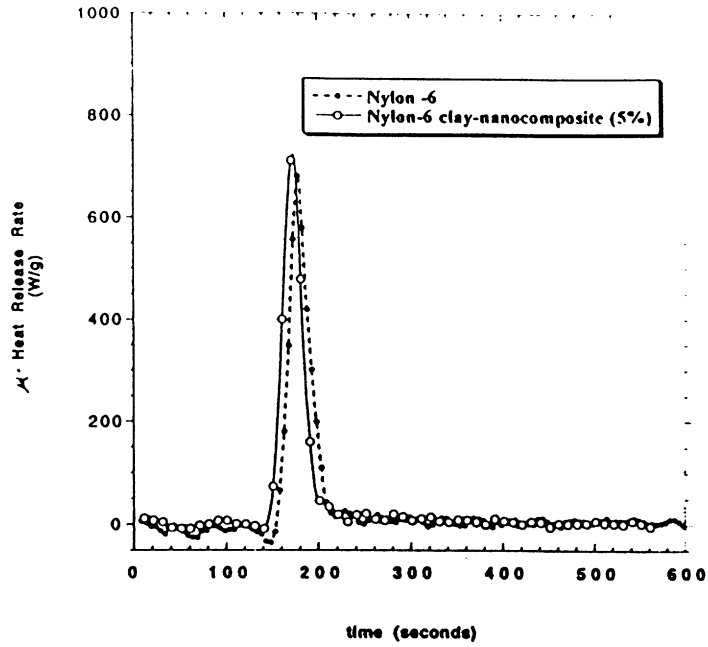


Figure 6. Microscale Combustion Calorimeter data for nylon-6 and the nylon-6 clay-nanocomposite (5 %).

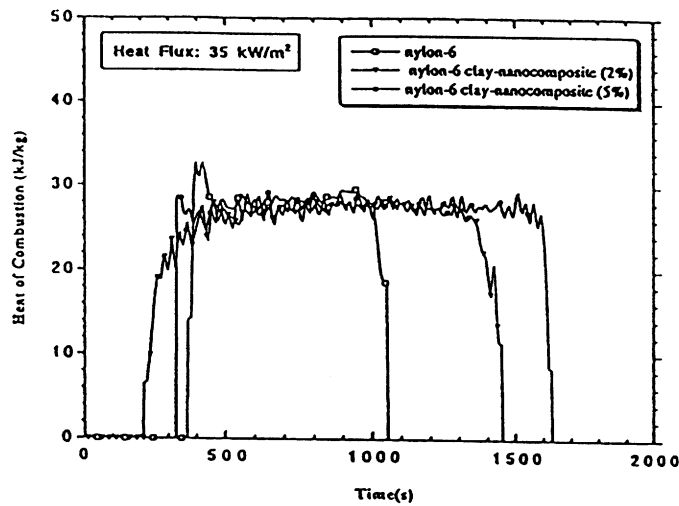


Figure 7. Comparison of the Heat of combustion (H_C) for the nylon-6 clay-nanocomposites and nylon-6. This data indicates that the clay-nanocomposite is not effecting the gas phase combustion of the nylon-6.

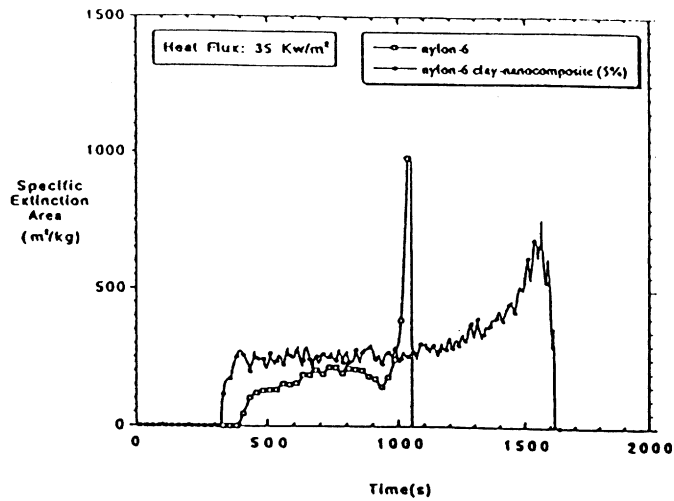


Figure 8. Comparison of the specific extinction area (SEA) data (a measure of soot) for nylon-6 and nylon-6 clay-nanocomposite (5 %). The nanocomposite has about a 50 % greater mean SEA than pure nylon-6 (also see Table 1).

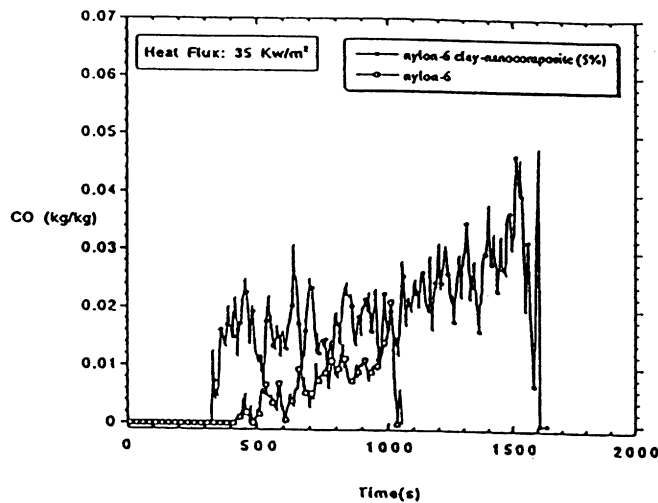


Figure 9. Comparison of the CO yield data for nylon-6 and nylon-6 clay-nanocomposite (5 %). A factor of two increase is observed in the CO yield for the nanocomposite (also see Table 1).

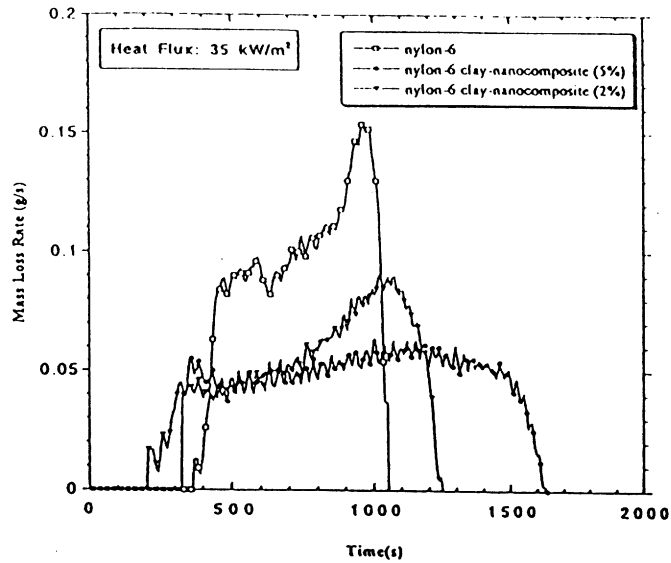


Figure 10. The mass loss rate data for nylon-6, nylon-6 clay-nanocomposite (2%), and nylon-6 clay-nanocomposites (5%). The three curves closely resemble the HRR curves (Figure 3), indicating that the reduction in HRR for the nanocomposites is primarily due to the reduced mass loss rate and the resulting lower fuel feed rate to the gas phase.

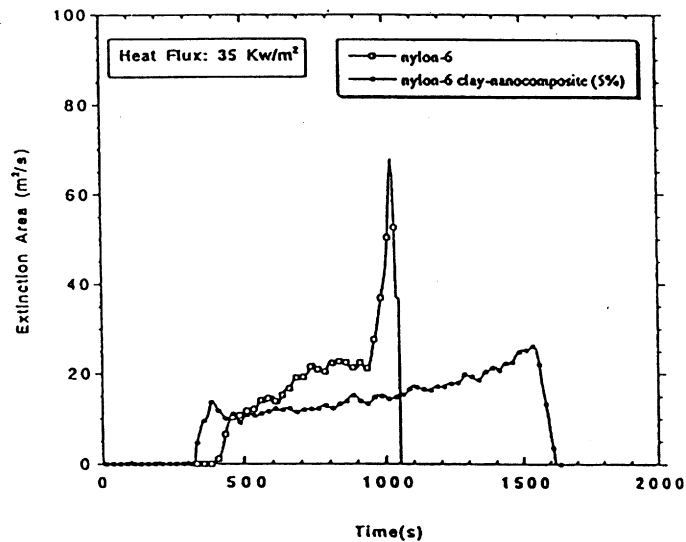


Figure 11. The extinction rate (m^2/s) data, obtained from the product of the SEA (m^2/kg) and the mass loss rate (kg/s). The lower mass loss rates give lower rates of soot generation for the nanocomposites.

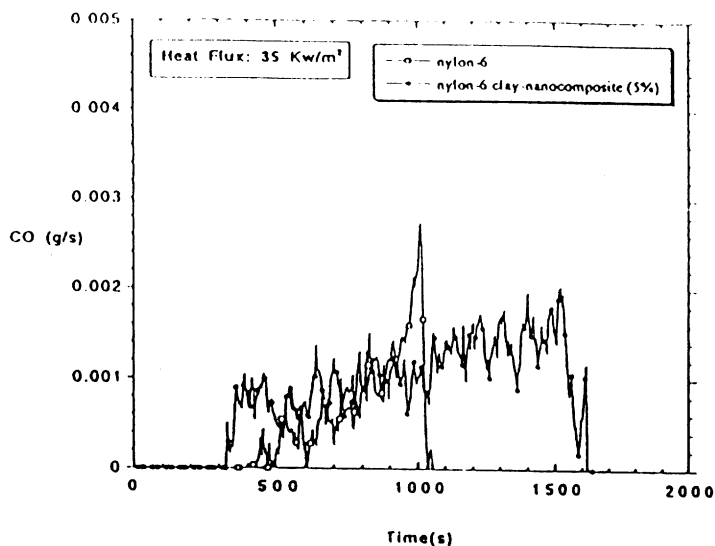


Figure 12. The CO production rate (kg/s) data, obtained from the product of the CO yield (kg/kg) and the mass loss rate (kg/s). The lower mass loss rates give similar rates of CO generation during the combustion of the nanocomposites, as compared to the pure nylon.

References

1. S. Levchik, G. Camino, L. Costa, and G. Levchik, *Fire and Materials*, **19**, 1 (1995).
2. A. Hochberg, *Proceedings of the Fall FRCA Meeting*, Naples, FL., 159 (1996).
3. A. Usuki, Y. Kojima, M. Kawasumi, A. Okada, Y. Fukushima, T. Kurauchi, and O. Kamigaito, *J. Mater. Res.* **8**, 1179 (1993).
4. E. Giannelis, *Adv. Mater.* **8**, 29 (1996).
5. Y. Kojima, A. Usuki, M. Kawasumi, A. Okada, Y. Fukushima, T. Kurauchi, and O. Kamigaito, *J. Mater. Res.* **8**, 1185 (1993).
6. Certain commercial equipment, instruments, materials, services or companies are identified in this paper in order to specify adequately the experimental procedure. This in no way implies endorsement or recommendation by NIST.
7. V. Babrauskas, R. Peacock, *Fire Safety Journal*, **18**, 255 (1992).
8. V. Babrauskas, *Fire and Materials*, **19**, 243 (1995).
9. A. Marchal, et al., *Polymer Degradation and Stability*, **44**, 263 (1994).
10. E. Giannelis, and P. Messersmith, *J. Polym. Sci. A: Polym. Chem.*, **33**, 1047 (1995).
11. R. Lyon, R. Walters, *NISTIR 5904*, Ed. K. Beall, 89 (1996).
12. M. Barnes, P. Briggs, M. Hirschler, A. Matheson, and T. O'Neill, *Fire and Materials*, **20**, 1 (1996).
13. B. Harwood, and J. Hall, *Fire J.* **83**, 29, (1989).
14. A. Hamins, D. Anderson, and H. Miller, *Combust. Sci. and Tech.*, **71**, 175 (1990).
15. P. Hornsby, J. Wang, R. Rothon, G. Jackson, G. Wilkinson, and K. Cossick, *Polymer Degradation and Stability*, **51**, 235 (1996).
16. I. Wan, J. McGrath, and T. Kashiwagi, in "Fire and Polymers II" G. Nelson, Ed., ACS Symposium Series **599**, American Chemical Society, Washington, DC (1995).
17. M. Le Bras, S. Bourbigot, *Fire and Materials*, **20**, 39 (1996).
18. reference 4 and R. Vaia, K. Jandt, E. Kramer, and E. Giannelis, *Macromolecules*, **28**, 8080 (1995).